Preprint
UCRL-CONF-154933

PREDICTING THE EQUILIBRIUM DEUTERIUM-TRITIUM FUEL LAYER THICKNESS PROFILE IN AN INDIRECT-DRIVE HOHLRAUM CAPSULE

Jorge J. Sanchez and Warren H. Giedt

This article was submitted to the 15th Target Fabrication Conference, Gleneden Beach, Oregon, June, 1-5, 2003

U.S. Department of Energy

Lawrence
Livermore
National
Laboratory

10-27-2003

Approved for public release; further dissemination unlimited

DISCLAIMER

This document was prepared as an account of work sponsored by an agency of the United States Government. Neither the United States Government nor the University of California nor any of their employees, makes any warranty, express or implied, or assumes any legal liability or responsibility for the accuracy, completeness, or usefulness of any information, apparatus, product, or process disclosed, or represents that its use would not infringe privately owned rights. Reference herein to any specific commercial product, process, or service by trade name, trademark, manufacturer, or otherwise, does not necessarily constitute or imply its endorsement, recommendation, or favoring by the United States Government or the University of California. The views and opinions of authors expressed herein do not necessarily state or reflect those of the United States Government or the University of California, and shall not be used for advertising or product endorsement purposes.

This is a preprint of a paper intended for publication in a journal or proceedings. Since changes may be made before publication, this preprint is made available with the understanding that it will not be cited or reproduced without the permission of the author.

This report has been reproduced directly from the best available copy.

Available electronically at http://www.doc.gov/bridge

Available for a processing fee to U.S. Department of Energy
And its contractors in paper from
U.S. Department of Energy
Office of Scientific and Technical Information
P.O. Box 62
Oak Ridge, TN 37831-0062
Telephone: (865) 576-8401
Facsimile: (865) 576-5728
E-mail: reports@adonis.osti.gov

Available for the sale to the public from
U.S. Department of Commerce
National Technical Information Service
5285 Port Royal Road
Springfield, VA 22161
Telephone: (800) 553-6847
Facsimile: (703) 605-6900
E-mail: orders@ntis.fedworld.gov
Online ordering: http://www.ntis.gov/ordering.htm

OR

Lawrence Livermore National Laboratory
Technical Information Department's Digital Library
http://www.llnl.gov/tid/Library.html

PREDICTING THE EQUILIBRIUM DEUTERIUM-TRITIUM FUEL LAYER THICKNESS PROFILE IN AN INDIRECT-DRIVE HOHLRAUM CAPSULE

Jorge J. Sanchez and Warren H. Giedt
University of California/Lawrence Livermore National Laboratory
P. O. Box 808, Livermore, CA 94550

A numerical procedure for calculating the equilibrium thickness distribution of a thin layer of deuterium and tritium on the inner surface of an indirect drive target sphere (~ 2.0 mm in diameter) is described. Starting with an assumed uniform thickness layer and with specified thermal boundary conditions, the temperature distribution throughout the capsule and hohlraum (including natural convection in the hohlraum gas) is calculated. Results are used to make a first estimate of the final non-uniform thickness distribution of the layer. This thickness distribution is then used to make a second calculation of the temperature distribution with the same boundary conditions. Legendre polynomial coefficients are evaluated for the two temperature distributions and the two thickness profiles. Final equilibrium Legendre coefficients are determined by linear extrapolation. From these coefficients, the equilibrium layer thickness can be computed.

I INTRODUCTION

The indirect-drive targets for fusion testing in the National Ignition Facility (NIF)[a] will consist of a spherical capsule centrally mounted in a vertical circular cylinder or hohlraum. A generic[1] target is illustrated in Fig. 1. The fuel is a 50-50 atomic% deuterium-tritium mixture contained in a thin solid layer on the inner surface of a thin-walled spherical capsule. The capsule is mounted between thin plastic films. Heat released during tritium decay flows from the fuel layer, through the capsule wall and then to the hohlraum wall through a 50-50 mole% mixture of H_2 and He, which serves as a tamping gas. Also included in Fig. 1 are equalizer rings around each end of the hohlraum. These devices are needed to assure that heat flow in the hohlraum wall is parallel to the vertical axis. This is achieved by channeling the heat flow through many equal-thermal-resistance paths in the equalizers[2]. Heat is transferred through small-diameter sapphire or aluminum support rods to a liquid-helium-cooled heat sink. This target assembly is positioned at the center of the 10-meter diameter NIF target containment chamber.

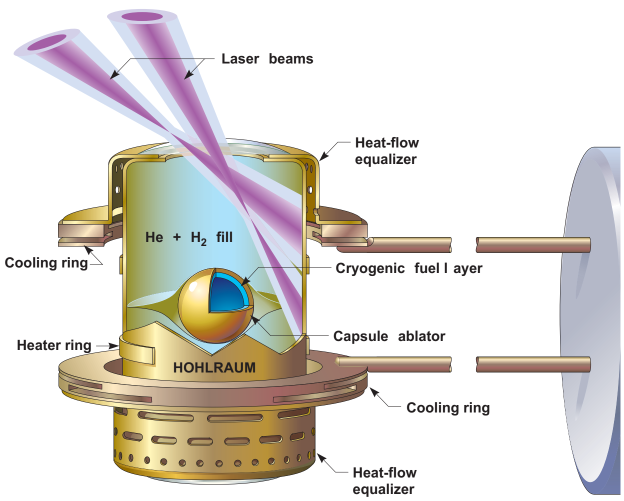

Fig. 1. A generic NIF target hohlraum unit.

An essential target requirement is that the solid layer of deuterium and tritium (D-T) be uniform in thickness. When this condition is satisfied the outward flow of heat released during tritium decay in the D-T layer will be spherically symmetric. Conversely, thermal effects within the hohlraum that prevent a spherically symmetric heat flow from the capsule surface will cause a non-uniform layer. The polar-angle-dependent distance from the capsule to the hohlraum wall is one such effect. In two previous studies[3,4] the D-T layer thickness was assumed to be uniform, and attention focused on finding appropriate boundary conditions which would decrease the heat flow through the H_2-He gas to the hohlraum wall in the mid-plane region. The first study[3] assumed conduction heat transfer only. An important result was that uniform auxiliary heating or heating over a short length on the outer surface of the hohlraum in the mid-plane region was sufficient to cause the heat flow from the D-T layer to be close to spherically symmetric. The second study[4] included natural convection in the hohlraum gas, the effects of which were found to be

[a] Currently being constructed at the Lawrence Livermore National Laboratory. The NIF will be a 192 beam frequency-tripled Nd:glass laser system with on-target energy and power of 1.8 MJ and 500 TW, respectively.

significantly different in the upper and lower gas regions. Trends, attributable to local convective heat transfer variation, were similar to results reported by Chatain and Vallcorba [5]. With an assumed uniformly thick D-T layer the inner ice surface temperature increased by as much as 3.0 mK from the bottom to the top of the capsule with hohlraum end temperatures of 19.5 K and auxiliary heating of 1.3 mW/mm^2 around the outer hohlraum wall above and below the mid-plane. In actuality, such a temperature difference would lead to a redistribution of the ice[6,7] by evaporation and recondensation of D-T until it had a uniform surface temperature . The resulting ice geometry would be far from uniform.

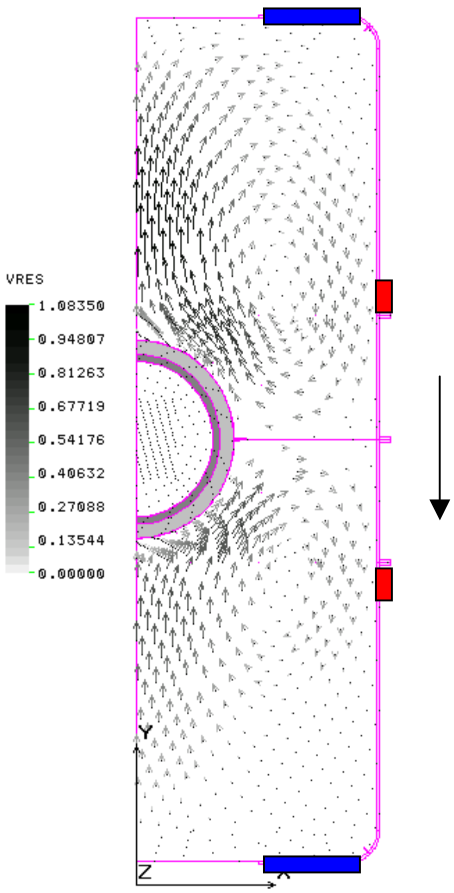

Fig. 2. Convection flow within a 2-region target model with cooling ring (horizontal rectangular areas) temperature of 19.5 K and side heating (small rectangles) of 1.3 mW/mm^2. The Direction of gravity is indicated by the arrow.

Although it may still be possible to use a trial and error procedure to find an appropriate set of boundary conditions for which the inner D-T surface temperature is uniform, with convection in the transfer gas the process is more complicated[8]. Being able to predict the D-T layer profile for a given set of boundary conditions is required for better efficiency in deciding how to modify the boundary conditions. In addition, an accurate description of the actual thickness profile is required for evaluating experimental results.

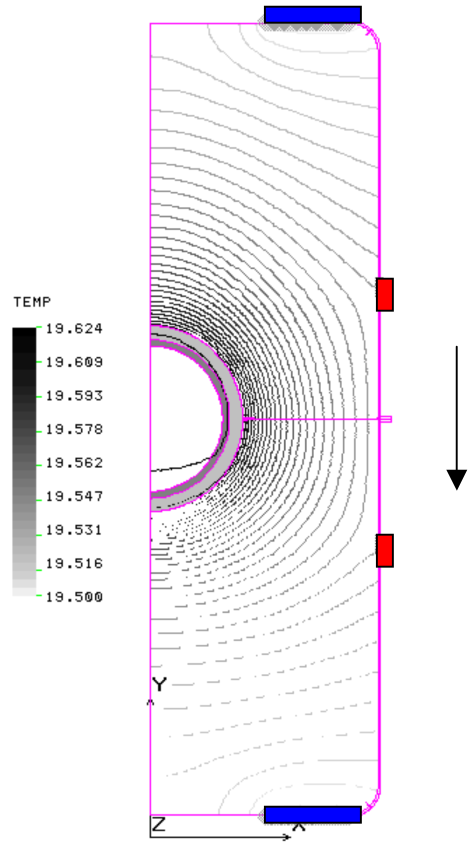

Fig. 3. Hohlraum temperature distribution for the 2-region model with convection in the heat transfer gas. Boundary conditions: cooling ring temperature of 19.5 K and side heating of 1.3 mW/mm^2

II FLUID FLOW AROUND AND HEAT TRANSFER FROM A CAPSULE IN A HOHLRAUM.

The current technique for mounting a capsule target in a hohlraum is between two supporting films shrunk around the capsule. This is illustrated in Fig. 2, which shows the capsule mounted at the mid-plane between two Formvar films[b] each on the order of 50 to 100 nanometers thick. With the capsule located at the center of the hohlraum the combination of capsule and hohlraum will

[b]Formvar is a polyvinyl resin marketed by the Monsanto Chemical Co. Films were formed by suspending a microscope slide vertically in a solution of Formvar and methylene-chloride. As the solution level is lowered a thin layer on the order of 50-80 nanometers thick forms on the slide surface. After the solvent has evaporated, the layer of Formvar is floated off the slide onto a water surface. It is then lifted off the water surface onto a wire ring larger in diameter than the diameter of the hohlraum.

be axially symmetric about the vertical axis. The system can therefore be modeled by zoning one side of a vertical section. A grid with quadrilateral elements was developed. Special attention had to be given to the thin mounting films because elements having a dimension less that 1 μm would be eliminated during the merging process. For this reason the films were specified as 3 μm thick and their thermal properties based on the fractions that were gas and plastic respectively. Fortunately, the thermal resistance of the films is very small, so that they had a negligible effect on thermal transfer. The final grid had over 43,000 elements with typical dimensions in the gas of 0.030 mm.

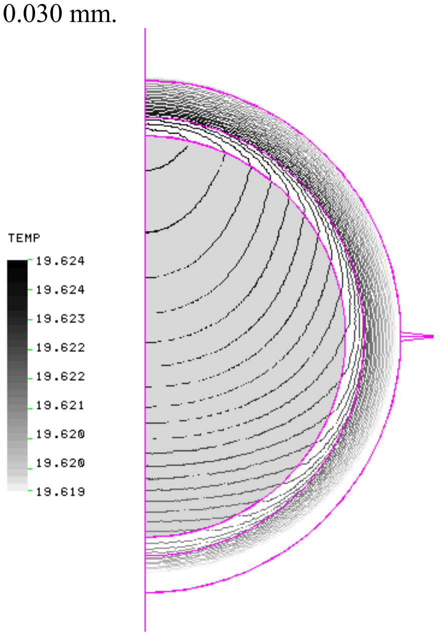

Fig. 4. Temperature distribution (0.15 K / isotherm) within the target capsule in a 2-region model shows a significant deviation (2.8 mK) from D-T inner surface uniformity due to the effect of convection

Although the grid is too detailed to show up in an overall plot, the capsule, gas regions, and hohlraum wall are clearly defined in Fig. 2. Also evident are the locations of the 0.75 mm wide strip heaters around the outside of the hohlraum about 1.4 mm above and below the mid-plane. The temperature at each end of the hohlraum was set to 19.5 K, and the heat flux from the strip heaters to 1.3 mW/mm^2. For these boundary conditions the COSMOS/M program was used to obtain numerical solutions of the momentum and energy equations[c]. Heat transfer drives the flows in Fig. 2 from the capsule towards cooling at each end of the hohlraum. The peak flow magnitude in the upper region is about twice that in the lower (around 1.1 mm/s compared to 0.5 mm/s). This is due to different effects of the heat transfer from the capsule. Above the capsule a decrease in density results in a buoyant force, which accelerates the gas vertically. In contrast, the density gradient produced in the gas below the capsule is stable.

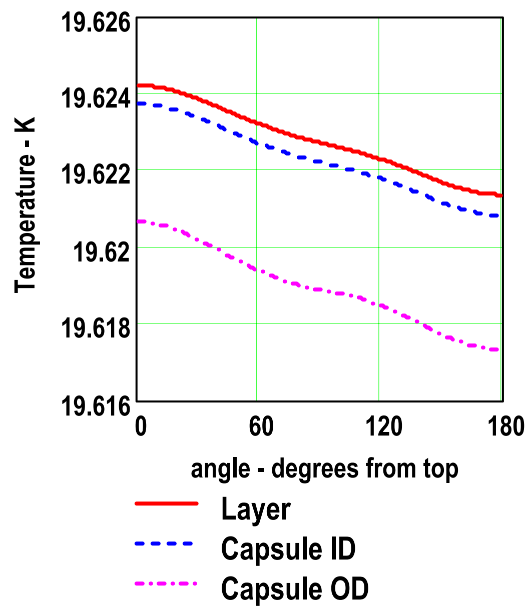

Fig. 5 Temperature distributions along the D-T layer inner surface, capsule ID, and capsule OD for the 2-region model with cooling ring temperatures of 19.5 K

In the upper region, gas flowing over the capsule separates from the capsule as it approaches the axis. The gas accelerates as it ascends and forms a plume. When it reaches the LEH, it slows down as it spreads radially outward to the hohlraum wall. Cooled by contact with the wall the gas density increases and descends toward the mid-plane. Since the wall temperature increases toward the mid-plane, the gas is heated, becomes more buoyant, and its downward velocity decreases. Before reaching the mid-plane, it turns toward the axis and flows over part of the top of the capsule.

In the lower region, a relatively broad column of gas approaches the capsule. As it turns toward the hohlraum wall, a boundary layer appears to develop along the capsule surface. The layer separates about 60^o from the bottom of the capsule center and flows toward the hohlraum wall. The gas is cooled as it flows down the

[c] Studies were carried out with the FLOWPLUS module recently incorporated into the COSMOS/M Finite Element Analysis Program[9]. The temperature variation throughout the capsule and hohlraum is on the order of 0.1 K so that constant mean property values can be assumed. At 19.5 K thermal conductivities (all in mW/mm K) were 8.0×10^{-2} for the D-T vapor[10], 0.294 for the D-T solid[11], 0.022 for the transfer gas[10,13], 0.15 for the assumed hydrocarbon capsule[12], and 1.0×10^{3} for the hohlraum[14]. The tritium decay heat release rates were 5×10^{-5} and 4.91×10^{-2} mW/mm^3 in the D-T vapor and solid respectively[10], and the transfer gas viscosity was 2.506×10^{-6} g/mm s[13]. Values for the density and specific heat capacity were taken from references 10 through 14.

wall. As the gas approaches the lower LEH the velocity decreases to where heat transfer is primarily by conduction. Gas further from the wall turns inward and gradually joins the upward buoyant flow toward the capsule.

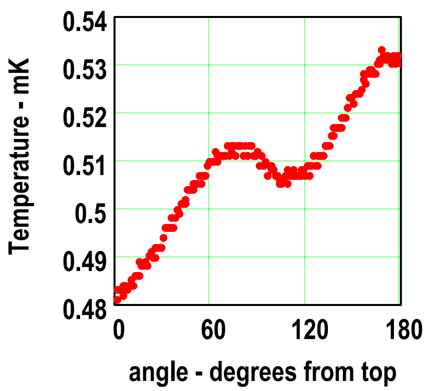

Fig. 6. Temperature difference between the D-T layer inner surface and the inner surface of the capsule for an assumed uniform thickness layer.

The temperature distribution for the above boundary conditions is shown by the isotherms plotted in Fig.3. Although the isotherms appear to be close to spherical around the capsule, the effect of the different convection patterns in the upper and lower regions causes the inner D-T surface temperature to be about 2.8 mK higher at the top than at the bottom (see Fig. 4). The distribution is shown more clearly in Fig.5, which also includes the temperature distributions around the inner and outer surfaces of the capsule. Since the top of the capsule is about 2.8 mK higher that the bottom, the overall temperature decrease from the capsule to the cooling ring is higher in the upper than in the lower region. This indicates that the total heat transfer in the lower region is slightly higher than in the upper region.

III ROCEDURE FOR ESTIMATING D-T LAYER THICKNESS PROFILE FORGIVEN BOUNDARY CONDITIONS

Surface temperature differences cause sublimation of D-T at high temperature locations and condensation at low temperature locations until the surface temperature achieves equilibrium. To reach a uniform surface temperature in equilibrium with its vapor, the D-T in a frozen layer in a capsule will distribute itself so that it is thickest where the resistance to heat flow from the capsule to the hohlraum is lowest and thinnest where the resistance to heat flow is highest. These locations were identified by the lowest and highest temperature decreases across an assumed uniformly thick D-T layer. The objective of this study was to derive a simple and rapid method for determining the amount by which the inner surface nodes had to be moved to achieve equilibrium..

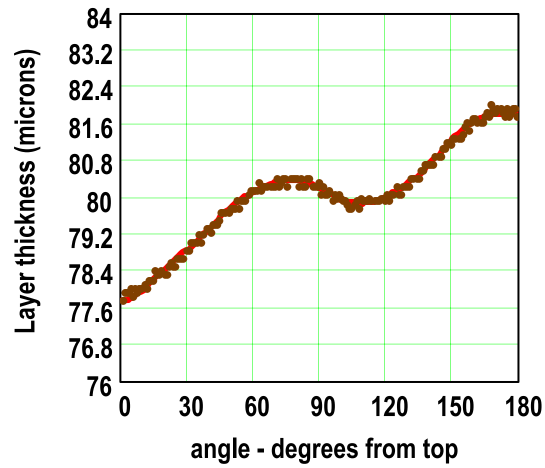

Fig. 7. D-T layer profile estimated (1st estimate) from the uniform thickness layer temperature drop assuming radial heat flow throughout the fuel layer.

The procedure developed involved the following four steps:

1) The radial temperature drop across the uniform thickness D-T layer with equal hohlraum end-temperatures (19.5 K) increases with angle θ from the vertical. As shown by the curve in Fig. 6 the temperature difference between the D-T surface and the inner capsule surface increases from 0.481 mK at the top to 0.532 mK at the bottom. We postulated that the magnitude of the radial heat flow at any angle θ from the vertical would be related to the local temperature decrease across the D-T layer[d].

2) With uniform volumetric heat generation g in the solid, the radial temperature distribution is governed by[15]

$$\frac{d}{dr}\left(\frac{r^2 dT}{dr}\right) = -\frac{g}{k_{DTS}} r^2 \qquad (1)$$

in which k_{DTS} denotes the thermal conductivity of the solid D-T. The tritium decay heat release rate in the vapor is negligible, so the temperature gradient at the inner D-T solid surface r_{DTi} is equal to zero. With the temperature at the outer ice surface as

[d] The possibility of using the temperature drop across the capsule wall was also investigated. The D-T layer change was selected because for a capsule wall of high thermal conductivity the temperature changes were small and difficult to determine precisely. This resulted in unacceptable scatter in new radius values.

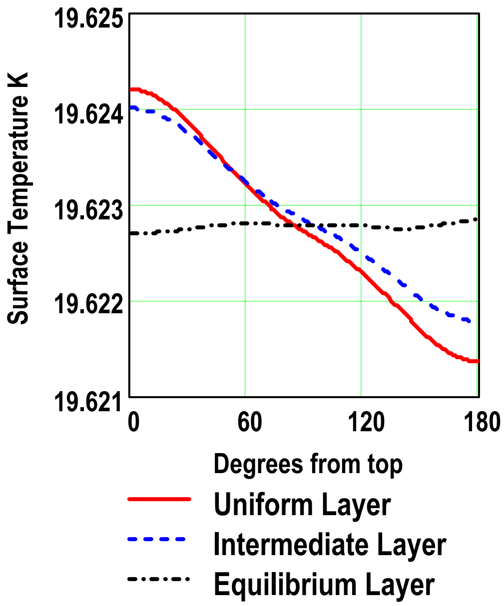

Fig. 8. The D-T layer inner surface temperature is a relative indicator of layer shape deviation. Ideally, after ice redistribution, the layer surface temperature would be uniform. The change between initial and intermediate values provides the slope for extrapolating to the final layer thickness distribution.

reference $(T = 0)$ the temperature decrease ΔT_{DT} across the layer is

$$\Delta T(\theta)_{DT} = \frac{g}{3k_{DTS}} \left[\frac{r_{ci}^{2} - r(\theta)_{l}^{2}}{2} + r(\theta)_{l}^{3} \left(\frac{1}{r_{ci}} - \frac{1}{r(\theta)_{l}} \right) \right] \quad (2)$$

$r(\theta)_l$ the radius of the inner D-T surface, and r_{ci} the outer radius equal to the inner capsule radius (thermal property values are given in footnote c). The initial inner radius r_l of the D-T is 0.87 mm; the capsule inner radius r_{ci} is 0.95 mm. The capsule wall thickness is 0.160 mm. Values of $\Delta T(\theta)_{DT}$ from θ = zero to 180° were substituted in Eq. (2) and an intermediate set of $r(\theta)_l$'s calculated, defining a new inner D-T surface. The changes from the uniform layer are approximately a few microns. Only the elements in the vapor and solid elements on either side of the interface are affected. Since these elements are about 20 μm thick, it was not necessary to rezone the model. The predicted layer thickness profile determined from the set of radii calculated from Eq. (2) is plotted in Fig. 7. As anticipated the layer is thinner at the top (~ 77.6 μm) and is thicker at the bottom (~ 81.8 μm).

3) The velocity and temperature distributions with the intermediate layer thickness shown in Fig. 7 are recalculated. The result for the inner D-T surface temperature is plotted in Fig. 8 along with the initial uniform thickness distribution surface temperature, and final equilibrium layer surface temperature. The temperature variation from the top to the bottom of

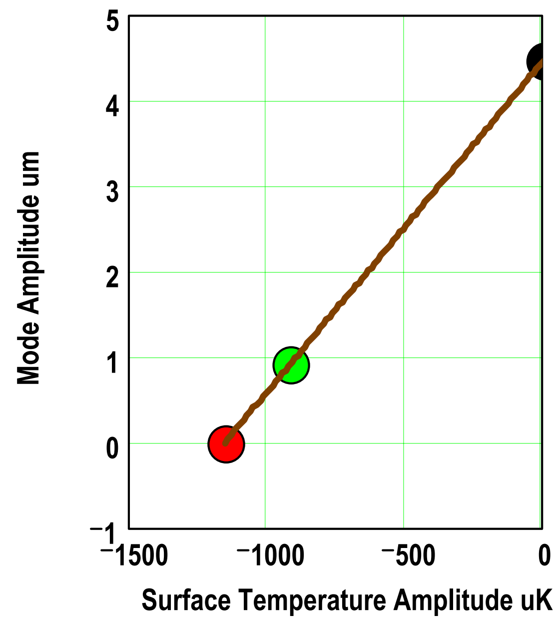

Fig. 9. Linear extrapolation procedure for each Legendre mode is demonstrated using mode one. Its initial amplitude of zero describes a uniform layer. The first estimate reduces the inner surface temperature some, but less than necessary. The extrapolated P_1 amplitude reduces this mode's contribution to the surface temperature to zero.

the ice layer has been reduced to about 2.0 mK from the uniform layer 2.9 mK.

4) The temperature and thickness data from the above steps are then used to extrapolate directly to an acceptable final layer thickness profile. The D-T layer profile and the inner surface temperature distribution are each represented by a series of Legendre polynomials. The procedure for determining the final equilibrium values of the amplitude of each polynomial is illustrated in Table 1 and Fig. 9.

III.A Legendre Polynomial Series for Layer Thickness Profile and Inner Surface Temperature Distribution

As modeled the D-T solid layer thickness profile and the inner surface temperature distribution are axially symmetric. Each can therefore be represented by a series of Legendre polynomials. Denoting the layer profile by $L(x)$ and the temperature distribution by $T(x)$, these are expressed by[17]

$$L(x) = \sum_{n=0}^{n=\infty} a_n P_n(x) \quad \text{and} \quad T(x) = \sum_{n=0}^{n=\infty} t_n P_n(x) \qquad (3)$$

in which the independent variable $x = \cos(\theta)$, and $P_n(x)$ is the Legendre polynomial of degree n, and the amplitudes of the individual terms are determined from

$$a_n = \frac{2n+1}{2}\int_{-1}^{+1} L(x)P_n(x)dx\,. \qquad (4)$$

Table 1 Legendre polynomial amplitudes for D-T layer thickness profiles and inner surface temperature distributions

Mode number	Uniform layer thickness profile - µm $L_u(x)$	Uniform layer surface temperature deviation - μK - $T_u(x)$	Layer thickness calculated from $\Delta T_{DT}(\theta)$ - μm - $L_{DT}(x)$	Surface temperature from $\Delta T_{DT}(\theta)$ thickness - μK - $T_{DT}(x)$	Linear Extrapolation to final layer thickness- μm - $L_{eq}(x)$
0	80	-10.84	80.08	-9.38	80.08
1	0.	-1154.76	0.91	-919.03	4.46
2	0	45.08	-0.1	36.93	-0.56
3	0	-267.86	1.19	-201.48	4.81
4	0	-9.21	0.03	-1.78	0.04
5	0	7.58	-0.14	10.11	0.41
6	0	6.07	-0.1	6.94	0.68
7	0	-4.8	0.06	-1.24	0.08
8	0	-0.01	-0.05	-5.5	-0.05
9	0	0.13	-0.05	0.2	0.09
10	0	0.99	-0.08	0.1	-0.09
11	0	0.86	0.04	1.37	-0.08
12	0	0.31	-0.03	-0.61	-0.01

For the initial uniform thickness D-T layer, $L(x) = L_u(x)$ is just the specified thickness of the layer, 80 µm. These values are listed in the second column of Table 1. Evaluation of the first 12 Legendre coefficients beyond the zero term for $L_u(x)$ and the corresponding ice surface temperature $T(x) = T_u(x)$ are listed in columns 2 and 3. Values listed in columns 4 and 5 are for the thickness profile determined by substituting $\Delta T_{DT}(\theta)$ in equation (2). The values in column 5 describe the inner surface temperature distribution obtained using the layer profile of column 4. The final column lists the amplitudes describing the equilibrium thickness profile, defined as that giving the ice surface temperature that is nearly isothermal. The extrapolation procedure for determining these values is illustrated for mode 1 in Fig. 9 from the data in Table 1

a) The data in columns 2 and 3 identify the initial point along the $a_n = 0$ axis with a value of $a_{1,init} = 0$, $t_{1,init} = -1154.76$.

b) The numbers in columns 4 and 5 identify a second point (the first estimate) with $a_{1,est} = 0.91$ and $t_{1,est} = -919.03$. These two points are used to establish the slope of the mode 1 curve as a function of t_1.

c) The intercept of this line with the $t_n = 0$ axis then yields the value of 4.46 μm for the equilibrium value of $a_{1,eq}$.

Applying a similar procedure to the other modes then yields a set of amplitudes for which the variation of the surface temperature distribution is near zero, as checked by the evaluation of T(x) with the 13 extrapolated Legendre coefficients. The amplitudes in the above Table are for a model with two gas regions, a transfer gas density of 2.0 mg/cm^3 and end temperatures of 19.5 K. A polar plot of the equilibrium thickness profile is presented in Fig. 10.

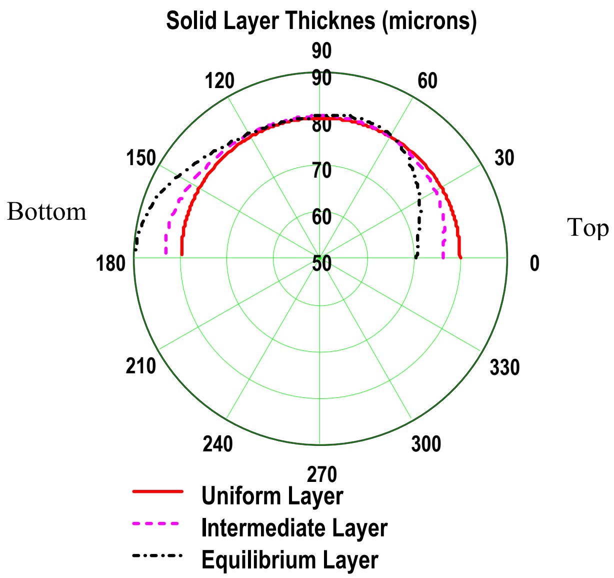

Fig. 10. Initial estimate and final values calculated for the layer thickness distribution. The corresponding layer inner surface temperature are shown in Fig. 8

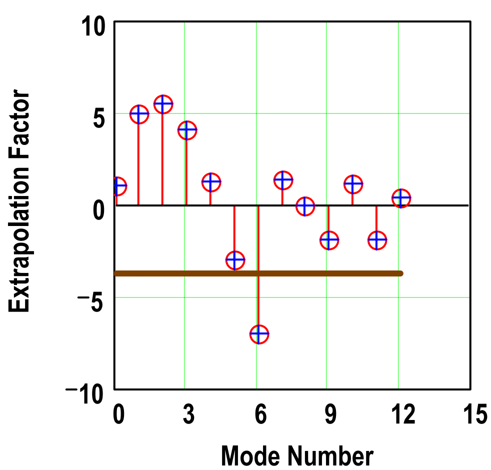

Fig. 11. Extrapolation factor is the ratio of the equilibrium layer modal amplitude to the amplitude of the first estimate of the non-uniform thickness layer. The horizontal line describes the change determined by extrapolating the standard deviation to zero

A Cartesian plot of the initial and predicted equilibrium D-T surface temperature distributions is shown in Figure 8. The layer thickness has decreased to about 70 μm at the top and increased to around 90 μm at the bottom. The surface temperature variation has been reduced from about 2.9mK to 125 μK.

As can be observed from the extrapolation for mode 1 in Figure 9, the amount of change in the intermediate value is relatively small compared to the extrapolated change required to achieve equilibrium. This is due to the fact that the circumferential heat flow from the top half to the bottom half of the capsule is small. The comparison can be expressed quantitatively by forming the ratios of the equilibrium layer thickness amplitudes to the intermediate layer thickness amplitudes. These ratios are plotted in Fig 11.

For comparative purposes the D-T layer thickness

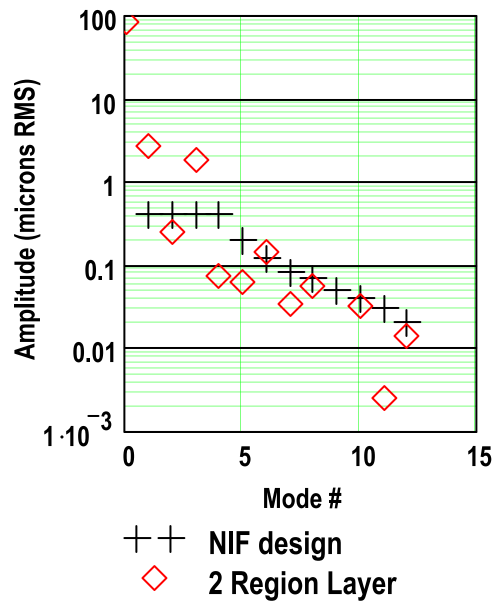

Fig. 12. RMS modal amplitudes for the 2-region model shows that convection increases modes 1 and 3 well beyond the NIF specifications for ignition

profile variation is expressed in terms of a Root-Mean-Square value or standard deviation σ determined from the variances of individual modes defined by:

$$\sigma_n^2 = \frac{1}{2}\int_{-1}^{+1}\left[a_n P_n(x)\right]^2 dx = \frac{a_n^2}{2}\int_{-1}^{+1} P_n(x)^2 dx \qquad (5)$$

However, since

$$\int_{-1}^{+1}\left[P_n(x)\right]^2 dx = \frac{2}{2n+1} \qquad (6)$$

then $$\sigma_n^2 = \frac{1}{2n+1} a_n{}^2 \qquad (7)$$

the standard deviation of a single mode σ_n is

$$\sigma_n = \sqrt{\frac{1}{2n+1}} a_n \quad (8)$$

and the standard deviation of the layer

$$\sigma = \sum_{1}^{n} \sqrt{\frac{1}{2n+1}} a_n \quad (9)$$

The summation is from 1 to n because $P_0(x)$ is the average constant value. The distribution of the standard deviation per mode of the D-T thickness profile in the 2-gas region model and a similar set of values for the NIF[18] are shown in Fig.12. The standard deviation determined from Eq. (9) is 3.3 μm. This value is about 6.5 times the NIF design specification. Fig. 12 shows that this high value is due primarily to large P_1 and P_3 amplitudes.

IV EQUILIBRIUM LAYER THICKNESS PROFILE FOR 5-GAS REGION MODEL

An important test of the prediction of layer thickness profile was to apply it to a model that would satisfy the

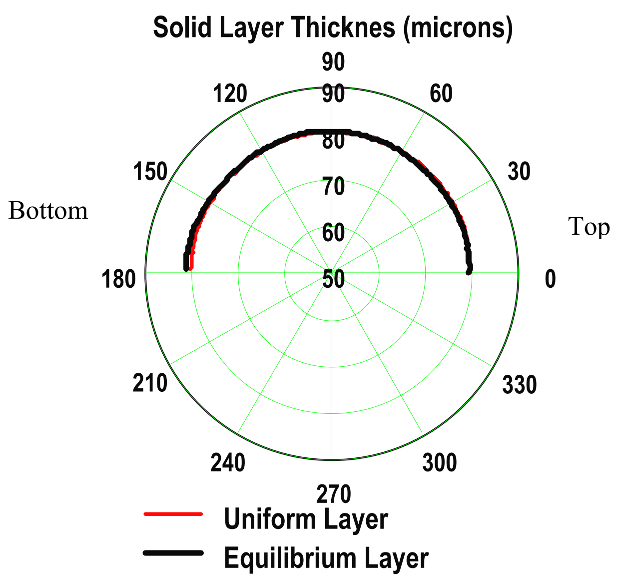

Fig. 13. Equilibrium layer thickness profile calculated for a five-region hohlraum. This curve shows that the layer thickness is indeed very close to 80 µm

NIF specifications. From a previous study[4] it had been found that by a) adding a thin films in the upper and lower halves of a hohlraum, convective heat transfer was significantly reduced, and by b) correcting the hohlraum end temperatures with offsets of ± 0.6 mK, the inner D-T surface temperature variation was reduced to around 125 µK. The equilibrium layer thickness profile calculated for these boundary conditions is plotted in Fig. 13. This curve shows that the layer thickness is indeed close to 80 µm. The layer asymmetry was predicted to be less than 0.5 μm RMS. NIF requirements specify a layer standard deviation of 0.43 μm. The comparison of the standard deviation per mode with those specified for a NIF target in Fig. 14 show that the 5-gas region model meets NIF specifications at all modes.

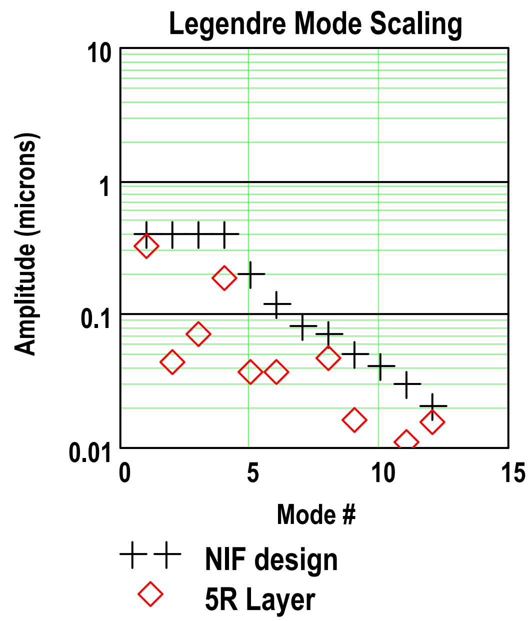

Fig. 14. Application of the procedure developed to the determination of equilibrium layer thickness profile for the 5-region model shows that the 5-region design meets the requirements for a NIF ignition target

V CONCLUSIONS

- A procedure has been developed for estimating the equilibrium solid D-T layer profile of a thermal CFD model for a specified set of boundary conditions. This is based on Legendre polynomial representation of distributions and multimode amplitude extrapolation.
- This procedure was validated by substituting the predicted layer profile into the COSMOS-FLOWPLUS program and obtaining a uniform layer surface temperature.
- Results are presented for a 2-gas region and a 5-gas region model. The 5-gas region model predicts a layer profile that meets the NIF specifications.

VI ACKNOWLEDGEMENT

This work was performed under the auspices of the U.S. Department of Energy by the UC, Lawrence Livermore National Laboratory under contract W-7405-EFG-48.

VII REFERENCES

1.J. LINDL, "Development of the Indirect-Drive Approach to Inertial Confinement Fusion and the Target Physics Basis for Ignition and Gain," Phys. Plasmas, **2**, 11, 3933 (Nov. 1995).

2. J. J. SANCHEZ, J. D. MOODY, W.H. GIEDT, and J. W. PIPES, "Multi-path Equalizer for Maintaining Uniform Azimuthal Heat Flow in a Cylindrical Hohlraum," Proceedings of 13th Target Specialist Conference, K. Schultz. Ed., General Atomics, San Diego (1999).

3. J. J. SANCHEZ and W. H. GIEDT, "Thermal Control of Cryogenic Cylindrical Hohlraums for Indirect-Drive Inertial Confinement Fusion," Fusion Technol., **36**, 11, 346-355 (1999).

4. J. J. SANCHEZ and W. H. GIEDT, "Thin Films for Reducing Tamping Gas Convection Heat Transfer Effects in a NIF Hohlraum," Fusion Technol., in press.

5. D. CHATAIN and R. VALLCORBA, "Experimental and Numerical Results in Closed Annular Space Heat Transfer at Low Temperature," Cryogenics, **37**, 4 ,187-193 (1997).

6. J. K. HOFFER, L.R. FOREMAN, E.R. MAPOLES, and J. D. SIMPSON, "Forming a Uniform Shell of Solid DT Fusion Fuel by the Beta-Layering Process," *Nucl. Fusion Research 1992*, **3**, p. 443, International Atomic Energy Agency, Vienna (1993).

7. T. P. BERNAT, E. R. MAPOLES, and J. J. SANCHEZ, "Temperature and Age Dependence of Redistribution Rates of Frozen Deuterium-Tritium," Inertial Confinement Fusion Quarterly Report, **1**, 2, p57, Lawrence Livermore National Laboratory (Jan.-Mar. 1991).

8. S. CHARTON, A. FABRE, and P. BACLET, "Cryogenic Indirect Drive Target—A Thermal Study," Fusion Technol., **38**,7, 156-160 (2000).

9. "COSMOS/M, Version 2.8," Structural Research and Analysis Corporation, 12121 Wilshire Blvd, Los Angeles, CA 90025-1170..

10. P. C. Souers, *Hydrogen Properties for Fusion Research*, p.106, University of California Press, Berkeley, California (1986).

11. G. W, Collins, P. C. Souers, E. M. Fearon, E. R. Mapoles, R. T. TSUGAWA, and J. R. GAINS, "Thermal Conductivity of Condensed D-T and T_2 ," *Phys. Rev. B*, **41**, 1816 (1993).

12. G. HARTWIG, *Polymer Properties at Room and Cryogenic Temperatures*, p. 110, Plenum Press, New York (1994).

13. R. D. MCCARTY, "*NBS TECHNICAL NOTE 631*, *Thermophysical Properties of Helium-4 from 2 to 1500 K with Pressures to 1000 Atmospheres*," U. S. Department of Commerce, National Bureau of Standards, Washington, D. C. 20234, Nov. 1972.

14. G. E. CHILDS, L. J. ERICKS, and R. L. POWEL, "Thermal Conductivity of Solids at Room Temperature and Below," COM-73-50843, p. 108, NBS (1973).

15. H. S. CARSLAW and J. C. JAEGER, *Conduction of Heat in Solids*, p. 230, 2nd ed., Oxford Press, London (1950).

16. "MATHCAD, Version 11," p. 304, Mathsoft, Inc., Cambridge, MA 02142.

17. G. ARTKEN, *Mathematical Methods for Physicists*, Academic Press (1995).

18. S. W. HAAN, Lawrence Livermore National Laboratory, Personnel Communication (2002).